TU Delft

Delft University of Technology

A 0.12mm^2 Wien-Bridge Temperature Sensor with 0.1°C (3σ) Inaccuracy from -40°C to 180°C

Pan, Sining; Gürleyük, Çagrı; Pimenta, Matheus F.; Makinwa, Kofi A.A.

DOI
10.1109/ISSCC.2019.8662457

Publication date
2019

Document Version
Final published version

Published in
2019 IEEE International Solid-State Circuits Conference, ISSCC 2019

Citation (APA)
Pan, S., Gürleyük, Ç., Pimenta, M. F., & Makinwa, K. A. A. (2019). A 0.12mm^2 Wien-Bridge Temperature Sensor with 0.1°C (3σ) Inaccuracy from -40°C to 180°C. In J. van der Spiegel (Ed.), *2019 IEEE International Solid-State Circuits Conference, ISSCC 2019* (Vol. 2019-February, pp. 184-186). Article 8662457 IEEE. https://doi.org/10.1109/ISSCC.2019.8662457

Important note
To cite this publication, please use the final published version (if applicable).
Please check the document version above.

Copyright
Other than for strictly personal use, it is not permitted to download, forward or distribute the text or part of it, without the consent of the author(s) and/or copyright holder(s), unless the work is under an open content license such as Creative Commons.

Takedown policy
Please contact us and provide details if you believe this document breaches copyrights.
We will remove access to the work immediately and investigate your claim.

This work is downloaded from Delft University of Technology.
For technical reasons the number of authors shown on this cover page is limited to a maximum of 10.

Green Open Access added to TU Delft Institutional Repository

'You share, we take care!' - Taverne project

https://www.openaccess.nl/en/you-share-we-take-care

Otherwise as indicated in the copyright section: the publisher is the copyright holder of this work and the author uses the Dutch legislation to make this work public.

10.3 A 0.12mm² Wien-Bridge Temperature Sensor with 0.1°C (3σ) Inaccuracy from -40°C to 180°C

Sining Pan, Çağrı Gürleyük, Matheus F. Pimenta, Kofi A. A. Makinwa

Delft University of Technology, Delft, The Netherlands

Resistor-based temperature sensors can achieve much higher resolution and energy efficiency than conventional BJT-based sensors [1], but they typically occupy more area (>0.25mm²) and have lower operating temperatures (≤125°C) [2-4]. This work describes a 0.12mm² resistor-based sensor that uses a Wien-bridge (WB) filter to achieve 0.1°C (3σ) inaccuracy from -40°C to 180°C. Compared to a state-of-the-art WB sensor [4], it occupies 6× less area and achieves comparable relative accuracy over a 76% wider operating range.

As shown in Fig. 10.3.1, the heart of the sensor is a Wien Bridge (WB) bandpass filter made from polysilicon resistors (R_{WB} = 64kΩ) and MIM capacitors (C_{WB} = 5pF). Unlike Wheatstone-bridge sensors [2,3], WB sensors only require one type of resistor, resulting in higher accuracy, and facilitating the experimental characterization of undocumented resistor properties such as 1/*f* noise and stress sensitivity. The filter is driven by a fixed-frequency square wave (f_{drive} = 500kHz) so that its temperature-dependent phase-shift ϕ_{WB} can be digitized by a phase-domain delta-sigma modulator (PDΔΣM) [3]. In the PDΔΣM, phase detection is performed by a chopper in the feedback loop of the 1st integrator (Fig. 10.3.2). Depending on the state of the bitstream BS, the chopper is driven by one of two reference phases $\phi_{0,1}$ (90°±30° w.r.t. to the phase of f_{drive}) such that the DC component of the integrated current is either positive or negative. The integration capacitor C_{int} must then be dimensioned to filter out the resulting ripple and ensure that the output of the 1st integrator does not clip. In [4], this required a 180pF capacitor that occupied more than half of the sensor's area.

To reduce the size of C_{int}, R_{WB} can be increased, but this will be at the expense of worse resolution. A better approach is to increase the output swing of the 1st integrator. In this work, the 1st integrator is built around a two-stage Miller-compensated opamp based on current-reuse amplifiers (Fig. 10.3.2). The 1st stage provides good energy efficiency, while the 2nd uses high-V_T devices to efficiently provide a near rail-to-rail output swing. Compared to the conventional choice of two common-source stages, the second stage provides twice the output current for the same bias current. Together with the doubling of R_{WB}, this allows the value of C_{int} to be reduced from the 180pF used in [4], to 23pF. At room temperature (RT), the amplifier draws 14μA and has a gain bandwidth product of 17MHz. To further reduce area, the 2nd integrator and the feed-forward coefficient are realized in a switched-capacitor manner, thus avoiding the large resistors used in [4]. The associated folded-cascode amplifier draws only 2.5μA at RT. On-chip logic generates the drive signal f_{ref} and the phase references $\phi_{0,1}$ from an external 6MHz frequency reference.

However, reducing C_{int} will increase the opamp's closed-loop input impedance Z_{in} ($\propto 1/(C_{int}\cdot GBW)$). This is in series with the WB and is thus a source of spread and 1/*f* noise. To minimize spread, a constant-Gm biasing circuit based on a resistor of the same type as R_{WB} ensures that Z_{in} tracks R_{WB} over a wide temperature range. Although the opamp is effectively chopped, the 1/*f* noise present in its bias current will modulate Z_{in}, and thus R_{WB}, causing residual 1/*f* noise. To minimize this, the core of the biasing circuit was realized with large PMOS devices (W/L = 40μm/5.5μm), and critical current mirrors were realized with the standard NPN transistors available in the chosen process (Fig. 10.3.2). Simulations show that the 1/*f* corner of the sensor is then about 1Hz and that R_{WB} is less than 1% of Z_{in} over corners.

Three pairs of identical sensors based on silicided p-poly (SP), unsilicided n-poly (NP) and high-resistive poly (HRP) resistors were fabricated on the same die in a 0.18μm CMOS process (Fig. 10.3.7). This facilitates the use of differential measurements to distinguish sensor drift from the inevitable ambient temperature drift. Each sensor consumes 29μA from a single 1.8V supply and occupies 0.12mm², of which the WB occupies 25%. PSDs of the bitstream outputs of the three sensors are shown in Fig. 10.3.3 (top) based on differential data captured during a 100s measurement interval. Figure 10.3.3 (bottom) shows the calculated resolution of each sensor versus conversion time. Due to its greater temperature coefficient (TC), the SP sensor exhibits the best resolution: 460μK in a 10ms conversion time, corresponding to a 110fJ·K² resolution FoM. For longer conversion times, sensor resolution is limited by 1/*f* noise. The corner frequencies are ~4Hz (NP and HRP), and ~1Hz (SP). However, the SP corner frequency is limited by the readout electronics.

10 chips (60 sensors) from a single batch were packaged in ceramic DIL and characterized from -40°C to 180°C. To correct for the inherent cosine nonlinearity of the PDΔΣM and the non-linear relationship between ϕ_{WB} and R_{WB} (Fig. 10.3.1, bottom), a 7th-order polynomial is used to translate the decimated output of each sensor into an equivalent sensor resistance R_{WB}. Since the temperature dependency of polysilicon resistors is comparatively linear, this approach minimizes the residual error after a 1st-order fit [4]. Figure 10.3.4 (top) shows the resulting temperature dependence of each resistor type. The following RT TCs were extracted: 0.31%/°C (SP), -0.15%/°C (NP) and -0.10%/°C (HRP), which agree with the process documentation. After a 1st-order fit to compensate for process spread, followed by the use of a fixed 6th-order polynomial to correct for the systematic non-linearity of the sensors, their residual spread is shown in Fig. 10.3.4 (bottom). The sensors achieve 3σ inaccuracies of 0.1°C (SP), 0.4°C (NP) and 0.9°C (HRP) from -40°C to 180°C. After a correlated 1-point trim [3], the SP sensor achieves an inaccuracy of 0.4°C (3σ), which is comparable with that of BJT-based sensors [5].

To observe the effects of mechanical stress, 10 chips from the same batch were characterized in injection-molded plastic QFN packages. Figure 10.3.5 (top) shows the average dependency of R_{WB} for both the ceramic and plastic packaged chips. After using the same non-linearity correction polynomials determined for the ceramic packaged chips, the inaccuracy after a 1st-order fit increases by only 0.2°C for the SP sensors, but to 1.4°C for the NP sensors, and even 2.5°C for the HRP sensors (Fig. 10.3.5 (bottom)). The sharp inflexion in all the inaccuracy plots around 100°C is probably due to the effects of moisture on the plastic packages [7]. Of the three resistor types, the SP resistor is clearly the least stress sensitive, exhibiting a packaging shift similar to that of BJT-based sensors [6].

In Fig. 10.3.6 the performance of the SP sensor is summarized and compared to the state-of-the-art. Compared to a state-of-the-art WB sensor [4], this design has a 76% larger operating range and occupies 6× less area. The latter is achieved at the expense of somewhat less relative inaccuracy [1]. Compared to a state-of-the-art WhB sensor [3], it achieves better accuracy and occupies 2× less area, but is less energy efficient. Measurements in plastic packages show that the SP sensors are quite insensitive to packaging stress (< 0.2°C packaging shift) and obtain good accuracy after a 1-point trim. They can thus replace BJT-based sensors in applications where both a wide temperature range and a high resolution are required.

Acknowledgments:
The authors would like to thank Zu-yao Chang for his help with the measurements, and the Advanced Packaging Center for expediting the plastic packaging.

References:
[1] K. A. A. Makinwa, "Smart Temperature Sensor Survey", [Online]. Available: http://ei.ewi.tudelft.nl/docs/TSensor_survey.xls
[2] C. H. Weng et al., "A CMOS Thermistor-Embedded Continuous-Time Delta-Sigma Temperature Sensor With a Resolution FoM of 0.65 pJ°C²," *IEEE JSSC*, vol. 50, no. 11, pp. 2491-2500, Nov. 2015.
[3] S. Pan and K. A. A. Makinwa, "A 0.25 mm²-Resistor-Based Temperature Sensor With an Inaccuracy of 0.12 °C (3σ) From -55 °C to 125 °C," *IEEE JSSC*, Oct. 2018.
[4] S. Pan et al., "A Resistor-Based Temperature Sensor with a 0.13pJ·K² Resolution FOM," *IEEE JSSC*, vol. 53, no. 1, pp. 163-174, Jan. 2018.
[5] K. Souri et al., "A 40μW CMOS Temperature Sensor with an Inaccuracy of ±0.4° C (3σ) from– 55° C to 200°C," *ESSCIRC*, pp. 221-224, Sept. 2013.
[6] B. Yousefzadeh et al., "A BJT-Based Temperature Sensor with a Packaging-Robust Inaccuracy of ±0.3°C (3σ) from -55°C to +125°C After Heater-Assisted Voltage Calibration," *ISSCC*, pp. 162-163, Feb. 2017.
[7] U. Ausserlechner et al., "Drift of Magnetic sensitivity of smart Hall sensors due to moisture absorbed by the IC-package," *IEEE Sensors*, pp. 455-458, Oct. 2004.

 978-1-5386-8531-0/19/$31.00 ©2019 IEEE

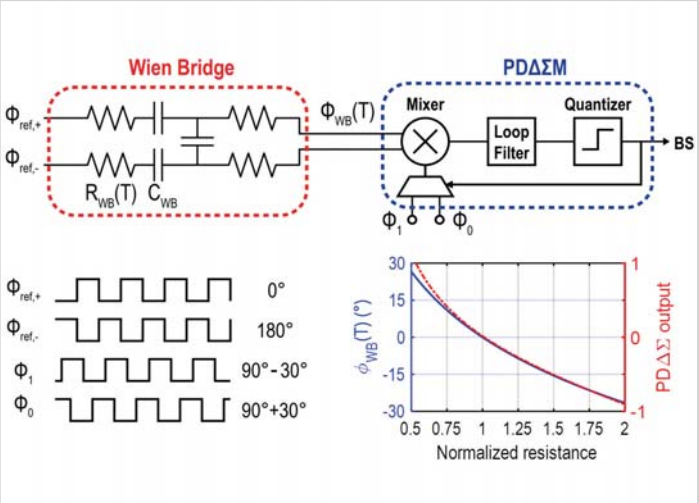

Figure 10.3.1: CTΔΣ readout of a Wien-bridge temperature sensor (top), waveforms, phase response of the Wien bridge and BS average of the PDΔΣM (bottom).

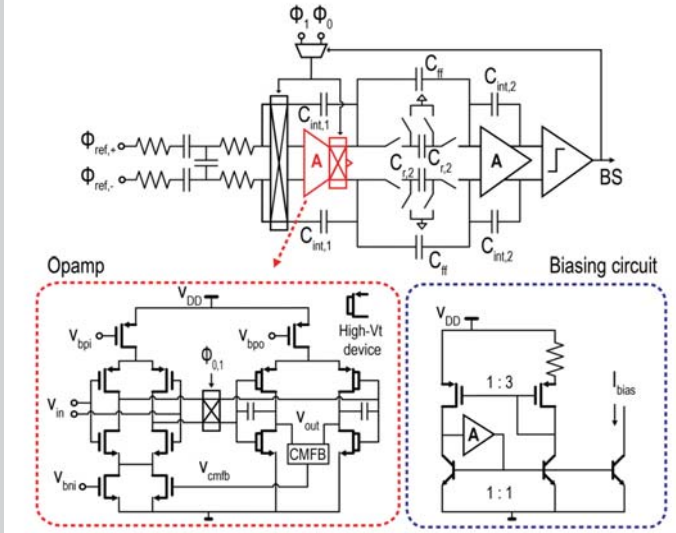

Figure 10.3.2: Block diagram of the PDΔΣM. Simplified diagram of the 1st-stage amplifier and the biasing circuit.

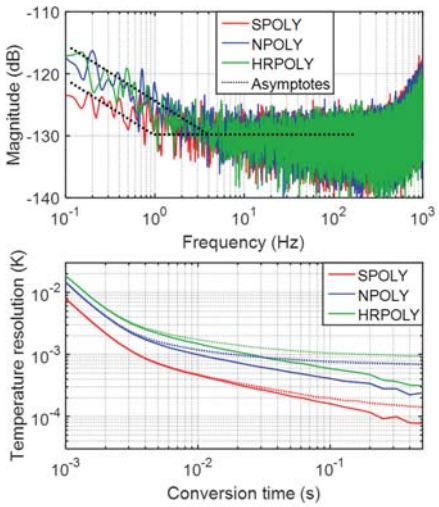

Figure 10.3.3: Bitstream spectra (100s interval, Hanning window) (top); Resolution vs. conversion time for 1s (solid lines) and 100s (dashed lines) intervals (bottom).

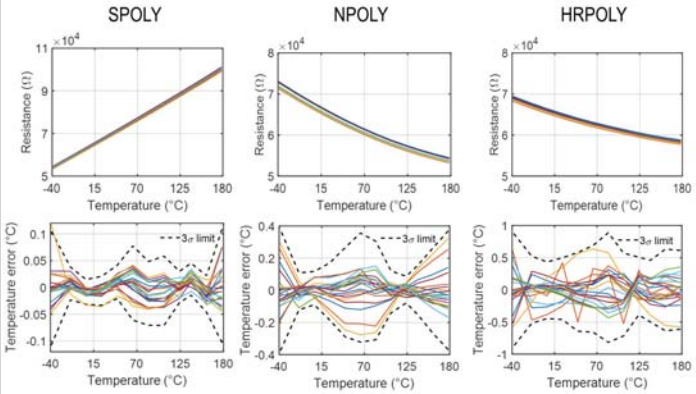

Figure 10.3.4: Extracted sensor resistance R_{WB} with ceramic packaging (top); Inaccuracy after a 1st-order fit and systematic non-linearity correction (bottom).

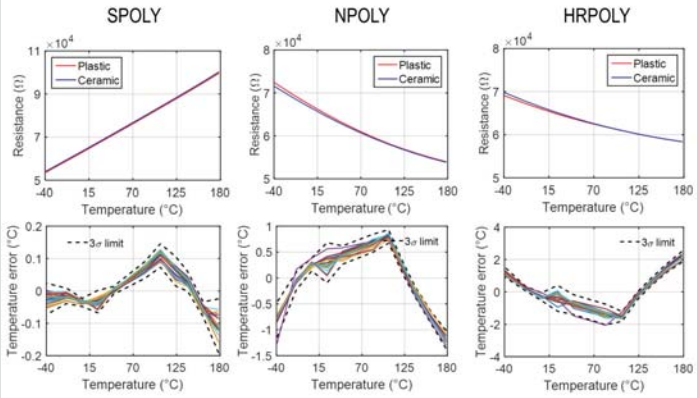

Figure 10.3.5: Average resistance vs. temperature of three types of resistors in different packages (top); Inaccuracy of plastic packaged sensors after a 1st-order fit and system non-linearity correction from ceramic packaged sensors (bottom).

	[2]	[3]	[4]	[5]	This Work	
Sensor type	Resistor WhB	Resistor WhB	Resistor WB	BJT	Resistor WB	
Technology	0.18µm	0.18µm	0.18µm	0.16µm	0.18µm	
Area [mm²]	0.43	0.25	0.72	0.1	0.12	
Temperature range	-40°C to 125°C	-55°C to 125°C	-40°C to 85°C	-55°C to 200°C	-40°C to 180°C	
Trimming points	2 [a]	2 [b]	2 [b]	1	1	2 [b]
3σ inaccuracy [°C]	0.4	0.12	0.03	0.4	0.4	0.11
Relative inaccuracy	0.48%	0.13%	0.05%	0.33%	0.36%	0.10%
Supply voltage [V]	1.5	1.8	1.8	1.6	1.8	
Power [µW]	65	94	160	35	52	
Conversion time [ms]	0.1	5	5	4.2	10	
Resolution [mK]	10	0.29	0.41	20	0.46	
Resolution FoM [fJ·K²] [c]	650	40	130	59000	110	

[a] 1-point trim and 1st-order fit. [b] 1st-order fit. [c] Energy / Conversion x (Resolution)².

Figure 10.3.6: Summary of measurement results and comparison with previous work.

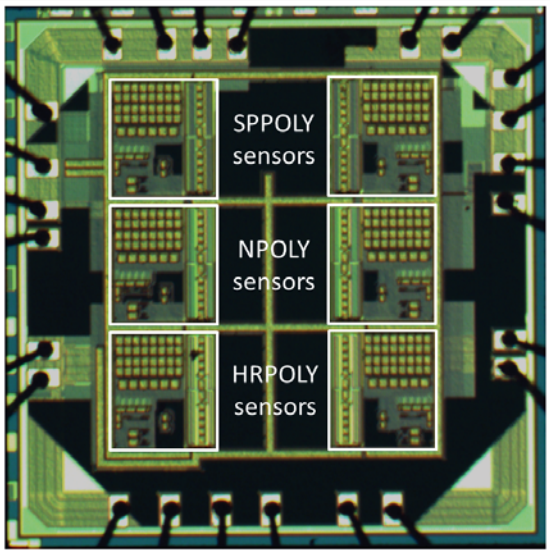

Figure 10.3.7: Micrograph of six temperature sensors on one die.

978-1-5386-8531-0/19/$31.00 ©2019 IEEE